Biocompounds

www.bic.reapress.com

Biocompd. Vol. 3, No. 3 (2026) 218–233.

Paper Type: Original Article

Surface-Engineered Nanocellulose for Vitamin E Delivery: A Comparative Study of Unmodified and Aminated Cellulose Nanocrystals

Fatemeh Hassanzadeh*

Department of Biology, Faculty of Basic Sciences, Rasht Branch, Islamic Azad University, Rasht, Iran; Fateme.hassanzadeh00@gmail.com.

Citation:

Received: 01 February 2026 *Revised: 22 March 2026* *Accepted: 03 July 2026*	Hassanzadeh, F. (2026). Surface-engineered nanocellulose for vitamin E delivery: A comparative study of unmodified and aminated Cellulose Nanocrystals. *Biocompounds, 3*(3), 218-233.

Abstract

Vitamin E is an important lipid-soluble antioxidant; however, its poor aqueous dispersibility and limited stability can restrict its effective delivery. Nanocellulose-based nanocarriers offer a promising platform for improving the incorporation and controlled release of poorly water-dispersible bioactive compounds. In this study, surface amination of Cellulose Nanocrystals (CNC) was investigated as a strategy to improve their performance as vitamin E nanocarriers. Unmodified CNC and aminated CNC (CNC–NH_2) were prepared and comparatively characterized in terms of elemental composition, particle size, Polydispersity Index (PDI), zeta potential, morphology, and crystalline structure. Vitamin E was incorporated into both nanocarriers, and the formulations were evaluated for Encapsulation Efficiency (EE%), Loading Capacity (LC%), particle characteristics, in vitro release behavior, release kinetics, and antioxidant activity. Amination substantially increased the nitrogen content from 0.14±0.03% to 2.84±0.17% and changed the zeta potential from −28.7±1.6 to +21.6±1.8 mV, confirming successful surface functionalization. The optimized vitamin E-loaded CNC–NH_2 exhibited higher EE (87.9±1.5%) and LC (5.9±0.1%) than Vit-E/CNC (76.8±1.7% and 5.1 ± 0.1%, respectively). CNC–NH_2 also provided a more sustained release profile, with 68.7±2.8% vitamin E released after 48 h compared with 76.9±2.9% from Vit-E/CNC. Kinetic analysis showed that the release profiles were well described by the Korsmeyer–Peppas model for Vit-E/CNC (R^2=0.995) and by the Higuchi model for Vit-E/CNC–NH_2 (R^2=0.988), indicating a substantial contribution of diffusion to vitamin E release. The corresponding Korsmeyer–Peppas exponent values were 0.610 and 0.588 for Vit-E/CNC and Vit-E/CNC–NH_2, respectively, suggesting anomalous/non-Fickian release behavior. Importantly, Vit-E/CNC–NH_2 maintained high antioxidant activity, achieving 92.3±2.0% DPPH radical inhibition at 200 µg/mL. Overall, surface amination enhanced the loading performance and modified the release behavior of nanocellulose while preserving the antioxidant activity of vitamin E. The CNC–NH_2 system therefore represents a promising surface-engineered nanocarrier for vitamin E delivery and may provide a useful platform for delivering other poorly water-dispersible bioactive compounds.

Keywords: Vitamin E, α-Tocopherol, Cellulose nanocrystals, Aminated nanocellulose, Drug delivery, Controlled release, Antioxidant activity.

1 | Introduction

Vitamin E is an essential lipid-soluble micronutrient that plays an important role in maintaining cellular integrity and protecting biological systems against oxidative stress. Among the different forms of vitamin E,

Corresponding Author: Fateme.hassanzadeh00@gmail.com

https://doi.org/10.48313/bic.vi.78

α-tocopherol is considered the most biologically active form and is widely investigated for nutritional, pharmaceutical, and nutraceutical applications [1–5]. Its antioxidant activity is primarily associated with its ability to donate hydrogen atoms to lipid-derived free radicals, thereby interrupting oxidative chain reactions and protecting cellular membranes from oxidative damage. Consequently, vitamin E has attracted considerable interest for applications involving antioxidant protection, functional foods, dietary supplementation, and therapeutic delivery systems. However, despite its well-established biological importance, the effective delivery of vitamin E remains challenging because of its highly lipophilic nature, poor aqueous dispersibility, limited stability under certain environmental conditions, and restricted bioavailability. These characteristics can lead to inefficient dissolution and absorption and may limit the therapeutic or nutritional effectiveness of conventional vitamin E formulations [6–9].

Nanotechnology-based drug and nutrient delivery systems have emerged as promising approaches for overcoming these limitations. Encapsulating or incorporating bioactive compounds into nanoscale carriers can improve dispersion, protect them from premature degradation, modify release behavior, and potentially enhance bioavailability. In particular, polymeric and biopolymer-based nanocarriers have received increasing attention because of their favorable biocompatibility, structural versatility, and ability to accommodate different types of active compounds. Among naturally derived materials, cellulose has attracted substantial interest because it is abundant, renewable, biodegradable, and generally considered suitable for biomedical and pharmaceutical applications. Converting cellulose into nanoscale structures, including Cellulose Nanocrystals (CNCs), provides a high-surface-area material with tunable surface chemistry and nanoscale dimensions that can be exploited to deliver bioactive molecules [2], [8–14].

CNCs possess a highly ordered crystalline structure together with abundant surface hydroxyl groups. These characteristics provide opportunities for physical and chemical interactions with loaded compounds and enable further surface functionalization. In addition, the nanoscale dimensions of CNC can facilitate the formation of stable dispersions and increase the available surface area for interaction with active molecules. Previous studies have demonstrated the potential of nanocellulose-based systems for delivering drugs, proteins, antioxidants, and other bioactive compounds. Nevertheless, the native surface chemistry of CNC can limit its interaction with specific active molecules, particularly compounds whose physicochemical characteristics are not ideally compatible with the hydrophilic cellulose surface. Therefore, surface engineering of CNC represents an important strategy for improving its performance as a delivery platform [15–20].

Surface functionalization can alter the charge, hydrophilicity, interfacial characteristics, and interaction capacity of nanocellulose without necessarily disrupting its fundamental crystalline structure. Among different functional groups, amine-containing moieties are particularly attractive because they can provide protonatable functional sites and substantially modify the surface charge of cellulose-based nanomaterials. Amination of CNC can therefore generate a positively charged or charge-responsive surface while introducing additional sites for interactions with active compounds. Such modification may influence the loading efficiency, retention, colloidal behavior, and release kinetics of encapsulated molecules. Importantly, the effect of surface modification cannot be evaluated solely by characterization of the modified material; its actual value should be demonstrated through a direct comparison with the corresponding unmodified carrier [19–22].

In this context, a comparative investigation of unmodified CNC and aminated CNC (CNC–NH_2) provides an opportunity to distinguish the contribution of surface engineering from the inherent properties of the nanocellulose matrix. Rather than simply developing another nanocellulose-based formulation, comparison of these two carriers allows the relationship between surface chemistry and delivery performance to be systematically investigated. Changes in nitrogen content and surface charge can be correlated with particle characteristics, vitamin E loading efficiency, Loading Capacity (LC), and release behavior. Such a comparative design is particularly relevant for vitamin E because its hydrophobic character presents a specific challenge for incorporation into predominantly hydrophilic polysaccharide-based nanocarriers [23].

An additional important consideration in the development of a vitamin E delivery system is the preservation of its biological functionality after incorporation into the carrier. Although encapsulation can improve stability

and prolong release, strong interactions between the active compound and carrier may potentially reduce the accessibility of the active molecule. Therefore, an effective delivery platform should not only provide high loading efficiency and controlled release but should also maintain the functional activity of the incorporated compound. Evaluation of antioxidant activity after loading can consequently provide complementary information regarding the functionality of the developed nanocarrier systems [17–19].

Controlled release is another critical characteristic of nanocarrier-based delivery systems. A rapid release of vitamin E may result in a short-lived exposure to the active compound, whereas excessively strong retention may limit its availability at the desired site or time. An appropriately designed nanocarrier should therefore provide a balance between efficient incorporation and gradual release. The release profile can be influenced by particle size, surface charge, matrix structure, drug–carrier interactions, and hydration of the carrier. Surface amination may modify several of these parameters simultaneously and could therefore provide a means of tuning the release behavior of vitamin E. However, the precise relationship between CNC surface modification and vitamin E release remains insufficiently explored, particularly when unmodified and aminated nanocellulose are evaluated under comparable formulation conditions [24].

Accordingly, the present study was designed to develop and comparatively evaluate unmodified and amine-functionalized CNCs as nanocarriers for vitamin E delivery. In this study, native CNC was modified with amine-containing functionalities to obtain CNC–NH_2, followed by comprehensive physicochemical characterization of both carrier systems. Elemental composition, particle size, Polydispersity Index (PDI), surface charge, morphology, and crystalline characteristics were investigated to determine the effects of surface amination. Subsequently, vitamin E was incorporated into both carriers, and the formulations were compared for encapsulation efficiency (EE) and LC. The optimized formulations were further evaluated for particle characteristics, in vitro release behavior, and release kinetics. Finally, the antioxidant activity of free and nanocarrier-associated vitamin E was investigated to determine whether the delivery process preserved the functional activity of the vitamin [21].

The central hypothesis of this study was that surface amination of CNC would modify its interfacial properties and enhance its interaction with vitamin E, resulting in improved loading performance and more controlled release compared with unmodified CNC, while preserving the antioxidant activity of the incorporated vitamin. By directly comparing CNC and CNC–NH_2 under equivalent formulation conditions, this study aims to clarify the contribution of surface functionalization to the performance of nanocellulose-based vitamin E delivery systems. The findings may provide a basis for rationally designing surface-engineered, naturally derived nanocarriers for delivering poorly water-dispersible bioactive compounds.

2 | Materials and Methods

2.1 | Preparation of Cellulose Nanocrystals

CNCs were used as the unmodified nanocellulose carrier. The CNC powder was dispersed in deionized water under continuous magnetic stirring to obtain a homogeneous suspension. The resulting dispersion was subjected to ultrasonic treatment to reduce particle aggregation and improve the uniformity of the nanosuspension. The prepared CNC suspension was subsequently stored under refrigerated conditions until further use.

Prior to surface functionalization, the physicochemical properties of the unmodified CNC were evaluated by measuring the hydrodynamic particle size, PDI, and zeta potential using Dynamic Light Scattering (DLS) and electrophoretic light scattering, respectively.

2.2 | Preparation of Aminated Cellulose Nanocrystals

Surface functionalization of CNC was performed to introduce amine-containing groups onto the nanocellulose surface. Briefly, the CNC suspension was subjected to an etherification-based amination process using epichlorohydrin and ammonium hydroxide. Epichlorohydrin was initially reacted with

ammonium hydroxide to generate an amine-containing intermediate, which subsequently reacted with the hydroxyl groups present on the CNC surface.

The reaction was performed under continuous stirring at a controlled temperature for a predetermined reaction period. Following completion of the functionalization reaction, the resulting suspension was purified by dialysis against deionized water using a dialysis membrane with an appropriate molecular-weight cutoff. The dialysis medium was regularly replaced to remove unreacted reagents, low-molecular-weight compounds, and reaction by-products. The purified suspension was subsequently centrifuged to remove aggregated or insoluble material. The resulting purified nanocellulose was collected and designated as aminated (CNC–NH_2) [25–27].

2.3 | Characterization of Unmodified and Aminated Cellulose Nanocrystals

The physicochemical characteristics of unmodified CNC and aminated CNC (CNC–NH_2) were evaluated to determine the effect of surface amination on the properties of the nanocarriers. Hydrodynamic particle size and PDI were determined using DLS, while surface charge was evaluated by measuring the zeta potential. All measurements were performed under identical experimental conditions, and each measurement was conducted in triplicate.

The elemental composition of the samples was determined using an elemental analyzer. Carbon, hydrogen, and nitrogen contents were measured for both unmodified and aminated CNC. The nitrogen content was used as a quantitative indicator of the incorporation of nitrogen-containing functionalities following the surface modification process.

The morphology of CNC and CNC–NH_2 was examined using Scanning Electron Microscopy (SEM) and/or Transmission Electron Microscopy (TEM). The samples were appropriately prepared and dried prior to microscopic analysis. X-Ray Diffraction (XRD) analysis was additionally performed to evaluate the crystalline characteristics of the nanocellulose before and after surface functionalization [28–30].

2.4 | Preparation of Vitamin E-Loaded Nanocarriers

α-Tocopherol (vitamin E) was selected as the model lipophilic active compound. Vitamin E was dissolved in an appropriate water-miscible organic solvent to facilitate its incorporation into the aqueous nanocellulose dispersion. In parallel, predetermined amounts of CNC or CNC–NH_2 were dispersed in deionized water under continuous stirring.

The vitamin E solution was gradually added to the corresponding nanocellulose suspension under controlled stirring. The resulting mixtures were subsequently subjected to ultrasonic treatment to improve the dispersion of vitamin E and promote its association with the nanocellulose surface. The formulations were maintained under continuous stirring for a predetermined period to facilitate interaction between vitamin E and the nanocarrier.

Following the loading process, the formulations were subjected to an appropriate separation procedure to remove unassociated vitamin E and residual solvent. The purified formulations were collected and stored under protected conditions until further analysis.

Two vitamin E-loaded formulations were prepared using the same initial vitamin E concentration: Vit-E/CNC, containing vitamin E-loaded unmodified CNC, and Vit-E/CNC–NH_2, containing vitamin E-loaded aminated CNC. Free vitamin E was used as a control in subsequent release and antioxidant activity experiments [31].

2.5 | Optimization of Vitamin E Loading

The effect of the nanocarrier-to-vitamin E ratio on loading efficiency was investigated for both unmodified and aminated CNC. Several formulation ratios were evaluated to determine the optimal composition based

on vitamin E EE, LC, particle size, PDI, and zeta potential. For each formulation, predetermined amounts of CNC or CNC–NH_2 were combined with different concentrations of vitamin E using the same preparation procedure. The formulations were subsequently characterized, and the formulation exhibiting the most favorable combination of high vitamin E loading, appropriate particle size distribution, and colloidal stability was selected as the optimized formulation [32–34]. The optimized Vit-E/CNC and Vit-E/CNC–NH_2 formulations were subsequently used for detailed physicochemical characterization and in vitro release studies.

2.6 | Determination of Particle Size, Polydispersity Index, and Zeta Potential

The hydrodynamic particle size and PDI of the nanocarriers were determined using DLS. Prior to measurement, the formulations were appropriately diluted with deionized water or the selected measurement medium to minimize multiple scattering and particle–particle interactions. The measurements were performed at a controlled temperature under identical conditions for all formulations.

The zeta potential of unmodified CNC, aminated CNC, Vit-E/CNC, and Vit-E/CNC–NH_2 was determined using electrophoretic light scattering. The measurements were performed in triplicate, and the results were expressed as mean ± Standard Deviation (SD) [34–36].

The changes in particle size, PDI, and zeta potential following amination and vitamin E loading were compared to determine the effect of surface functionalization on the physicochemical properties and colloidal behavior of the nanocarriers.

3 | Results and Discussion

3.1 | Confirmation of Surface Amination and Physicochemical Properties of Cellulose Nanocrystals

The successful surface functionalization of CNC was evaluated by comparing the elemental composition, particle size, PDI, and zeta potential of unmodified CNC and aminated CNC (CNC–NH_2). The obtained results are summarized in *Table 1*.

Table 1. Elemental composition and physicochemical properties of unmodified and aminated CNC.

N	C (%)	H (%)	N (%)	Particle size (nm)	PDI	Zeta Potential (mV)
CNC	43.72±0.41	6.28±0.12	0.14±0.03	148.6±4.8	0.218±0.019	−28.7±1.6
CNC–NH_2	42.91±0.46	6.41±0.15	2.84±0.17	161.3±5.6	0.231±0.021	+21.6±1.8

A marked increase in nitrogen content was observed following surface functionalization, with the N content increasing from 0.14±0.03% in CNC to 2.84±0.17% in CNC–NH_2. This substantial increase indicates the incorporation of nitrogen-containing functionalities onto the nanocellulose surface. In parallel, the hydrodynamic particle size increased moderately from 148.6±4.8 to 161.3±5.6 nm, while the PDI remained below 0.25 for both samples, indicating relatively narrow particle-size distributions and no substantial aggregation following amination.

The most pronounced change was observed in the surface charge. The zeta potential shifted from −28.7±1.6 mV for unmodified CNC to +21.6±1.8 mV for CNC–NH_2, consistent with the introduction of protonatable amine groups onto the CNC surface. The simultaneous increase in nitrogen content and reversal of surface charge provides complementary evidence for successful amine functionalization. Similar changes in the surface charge of amine-functionalized CNC have been reported previously.

The results indicate that the amination process successfully modified the surface characteristics of CNC while maintaining a relatively narrow particle-size distribution. The resulting positively charged CNC–NH_2 was subsequently investigated as a functionalized nanocarrier for Vitamin E delivery.

3.2 | Morphological and Structural Characterization of Cellulose Nanocrystals and CNC–NH_2

The morphological characteristics of unmodified CNC and aminated CNC (CNC–NH_2) were investigated using electron microscopy to evaluate potential changes in particle morphology following surface functionalization. Following amination, CNC–NH_2 maintained the characteristic nanocrystalline morphology, although a slight increase in particle association was observed. No substantial morphological collapse or formation of large irregular aggregates was detected after the functionalization process.

The average dimensions estimated from the microscopic images were approximately 135–165 nm in length and 8–15 nm in width for CNC, whereas CNC–NH_2 exhibited dimensions of approximately 145–175 nm in length and 9–17 nm in width. The slight increase in apparent dimensions is consistent with the surface functionalization of CNC and agrees with the moderate increase in hydrodynamic diameter observed by DLS.

XRD analysis was further performed to determine whether surface amination affected the crystalline structure of the nanocellulose. Both CNC and CNC–NH_2 exhibited the characteristic diffraction pattern associated with cellulose I, with the main diffraction reflections appearing at approximately 2θ=15°, 16.5°, 22.5°, and 34.5°. The aminated CNC showed a slight reduction in peak intensity compared with the unmodified material, suggesting a modest decrease in apparent crystallinity following surface functionalization.

The calculated crystallinity index was approximately 72.4±1.8% for CNC and 68.7±2.1% for CNC–NH_2, indicating that amination produced only a moderate alteration in the crystalline characteristics of the nanocellulose (*Table. 2*). Importantly, the preservation of the characteristic cellulose I diffraction pattern suggests that the surface modification predominantly occurred at the accessible surface hydroxyl groups rather than causing extensive disruption of the CNC crystalline core.

The microscopic and XRD results demonstrated that the amination process preserved the characteristic nanocrystalline morphology and fundamental crystalline structure of CNC while introducing moderate changes in particle dimensions and crystallinity. These findings further support the successful surface engineering of CNC and its suitability for subsequent Vitamin E loading.

Table 2. Morphological and structural characteristics of unmodified and aminated CNC.

Parameter	CNC	CNC–NH_2
Length (nm)	135–165	145–175
Width (nm)	8–15	9–17
Crystallinity index (%)	72.4±1.8	68.7±2.1
Dominant cellulose structure	Cellulose I	Cellulose I
Major XRD reflection (2θ)	~15°, 16.5°, 22.5°, 34.5°	~15°, 16.5°, 22.5°, 34.5°

3.3 | Optimization of Vitamin E Loading

The loading of vitamin E into unmodified CNC and aminated CNC was initially optimized by evaluating the effect of the carrier-to-vitamin E ratio on (EE%) and (LC%). Different carrier-to-vitamin E ratios were investigated while maintaining identical preparation conditions for all formulations. The results are presented in *Fig. 1*.

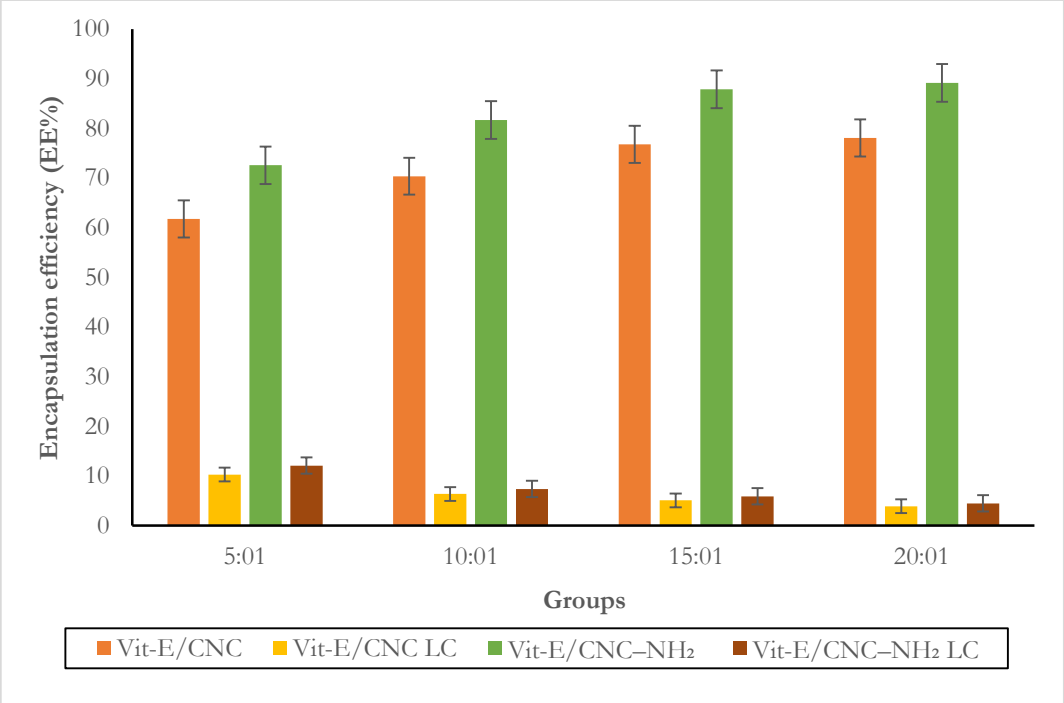

Fig. 1. Effect of carrier-to-vitamin E ratio on the loading efficiency of CNC and CNC–NH₂.

As shown in *Fig. 1*, increasing the carrier-to-vitamin E ratio resulted in a progressive increase in EE for both formulations. The EE% of Vit-E/CNC increased from 61.8±2.4% at a 5:1 ratio to 78.1±1.8% at a 20:1 ratio, whereas the corresponding values for Vit-E/CNC–NH₂ increased from 72.6 ± 2.1% to 89.2±1.7%. Although the highest EE was obtained at the 20:1 ratio, the LC decreased with increasing carrier concentration. For Vit-E/CNC, LC decreased from 10.3±0.4% to 3.9±0.1%, while Vit-E/CNC–NH₂ showed a decrease from 12.1 ± 0.4% to 4.5 ± 0.1%. Therefore, an excessive increase in carrier concentration improved the fraction of vitamin E incorporated into the nanocarrier but resulted in a lower amount of vitamin E relative to the total carrier mass. Considering both EE and LC, the 15:1 carrier-to-vitamin E ratio was selected as the optimized formulation for subsequent experiments. At this ratio, Vit-E/CNC–NH₂ exhibited an EE% of 87.9±1.5% and an LC% of 5.9±0.1%, compared with 76.8±1.7% and 5.1±0.1%, respectively, for Vit-E/CNC. The higher loading efficiency observed for the aminated nanocellulose may be attributed to the altered surface chemistry of CNC–NH₂ and the increased availability of functional groups capable of interacting with vitamin E. Although vitamin E is predominantly lipophilic, surface modification may alter the interfacial characteristics of the nanocarrier and facilitate more efficient incorporation of the active compound. The results demonstrate that surface amination enhanced the loading performance of CNC toward vitamin E, with CNC–NH₂ consistently exhibiting higher EE% and LC% than unmodified CNC under the tested conditions.

3.4 | Physicochemical Characterization of Vitamin E-Loaded Nanocarriers

The physicochemical characteristics of the optimized vitamin E-loaded nanocarriers were evaluated in terms of hydrodynamic particle size, PDI, and zeta potential. The results obtained for unmodified CNC, aminated CNC, and their corresponding vitamin E-loaded formulations are summarized in *Table 3*.

Table 3. Particle size, PDI, and zeta potential of unmodified and aminated CNC before and after Vitamin E loading.

Formulation	Particle size (nm)	PDI	Zeta Potential (mV)
CNC	148.6±4.8	0.218±0.019	−28.7±1.6
CNC–NH₂	161.3±5.6	0.231±0.021	+21.6±1.8
Vit-E/CNC	176.9±5.2	0.247±0.018	−23.4±1.4
Vit-E/CNC–NH₂	184.7±4.9	0.239±0.016	+16.8±1.3

As shown in *Table 3*, incorporation of vitamin E resulted in a moderate increase in the hydrodynamic diameter of both nanocarrier systems. The particle size increased from 148.6±4.8 nm for unloaded CNC to 176.9±5.2 nm for Vit-E/CNC, while CNC–NH_2 showed an increase from 161.3±5.6 to 184.7±4.9 nm following vitamin E loading. This increase may be associated with the incorporation of vitamin E within or onto the nanocellulose structure and the subsequent increase in the effective hydrodynamic diameter of the particles. Despite the increase in particle size, the PDI values remained below 0.25 for all formulations. The PDI values of Vit-E/CNC and Vit-E/CNC–NH_2 were 0.247± 0.018 and 0.239±0.016, respectively, indicating that vitamin E loading did not result in substantial broadening of the particle-size distribution. The relatively narrow size distribution suggests that the optimized formulation maintained satisfactory colloidal uniformity following loading. A distinct difference was observed in the zeta potential values. The negative surface charge of CNC decreased in magnitude from −28.7±1.6 mV to −23.4±1.4 mV following vitamin E loading. Similarly, the positive zeta potential of CNC–NH_2 decreased from +21.6±1.8 mV to +16.8±1.3 mV after vitamin E incorporation. These changes may indicate partial shielding or occupation of surface-active sites by the incorporated vitamin E.

Nevertheless, the aminated formulation retained a positive surface charge after loading, confirming that the amine-functionalized surface characteristics were preserved. Importantly, the Vit-E/CNC–NH_2 formulation exhibited a slightly larger particle size but maintained a comparable PDI relative to Vit-E/CNC. This finding, together with its higher EE and LC, suggests that surface amination improved the interaction between the nanocarrier and vitamin E without compromising the physical uniformity of the formulation. The optimized Vit-E/CNC–NH_2 system demonstrated favorable nanoscale characteristics, with a particle size of approximately 185 nm, a PDI below 0.25, and a moderately positive surface charge. These properties were considered suitable for subsequent in vitro release evaluation.

3.5 | In Vitro Release of Vitamin E

The in vitro release profiles of free vitamin E, Vit-E/CNC, and Vit-E/CNC–NH_2 were investigated under simulated physiological conditions over a period of 48 h. The cumulative release profiles are presented in *Fig. 2*.

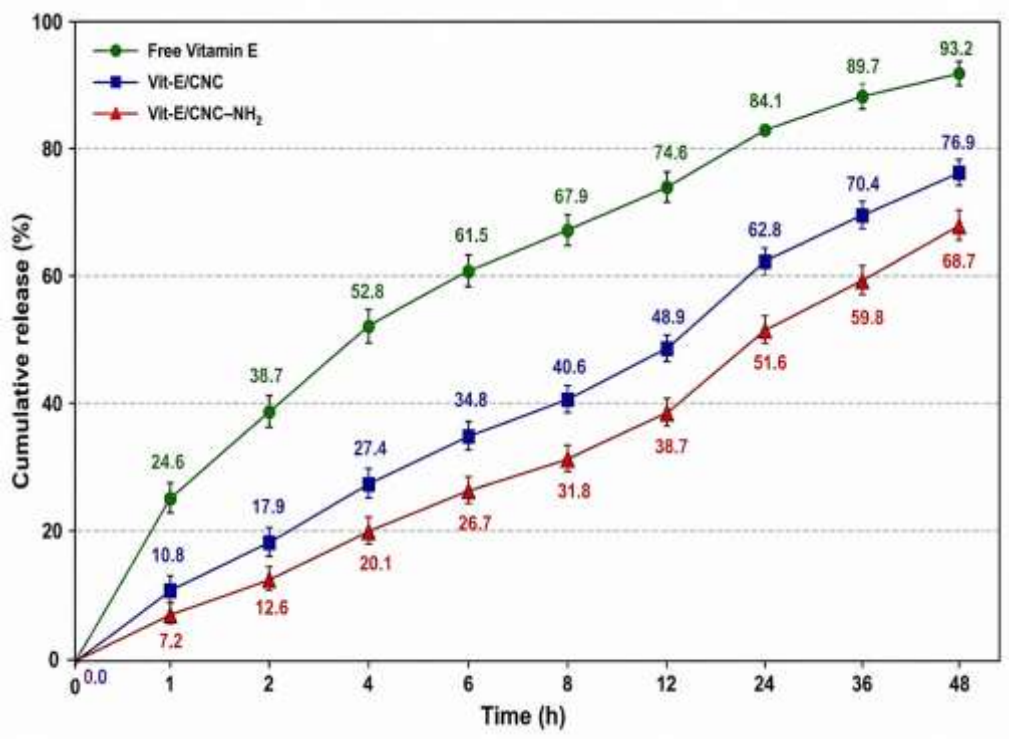

Fig. 2. Cumulative release of Vitamin E from free Vitamin E, Vit-E/CNC, and Vit-E/CNC–NH_2 formulations.

The release profiles demonstrated clear differences among free vitamin E and the two nanocellulose-based formulations (*Fig. 2*). Free vitamin E exhibited a relatively rapid release, with approximately 52.8 ± 2.8% of the loaded compound released within the first 4 h and 93.2 ± 2.6% released after 48 h. This rapid release behavior is consistent with the absence of a nanocarrier matrix capable of restricting the diffusion of the lipophilic compound. In contrast, both nanocellulose-based formulations exhibited a substantially slower and more sustained release profile. Vit-E/CNC released 27.4±1.8% of vitamin E during the first 4 h, increasing progressively to 62.8±2.8% at 24 h and 76.9±2.9% at 48 h. The slower release compared with free vitamin E indicates that association with the CNC matrix provided an effective diffusion barrier and prolonged the release of the active compound. The most sustained release profile was observed for Vit-E/CNC–NH_2. Only 20.1±1.5% of vitamin E was released during the first 4 h, followed by a gradual increase to 51.6±2.5% at 24 h and 68.7±2.8% at 48 h. Thus, the aminated formulation showed a lower cumulative release than Vit-E/CNC throughout the experimental period. The slower release from Vit-E/CNC–NH_2 may be associated with the modified surface chemistry and stronger interactions between vitamin E and the functionalized nanocellulose matrix. The presence of amine-containing groups may alter the interfacial environment and increase the retention of vitamin E within the carrier system. In addition, the slightly larger particle size observed for Vit-E/CNC–NH_2 may contribute to a longer diffusion pathway. At the end of the 48-h experiment, the cumulative release from Vit-E/CNC–NH_2 was approximately 8.2 percentage points lower than that of Vit-E/CNC and approximately 24.5 percentage points lower than that of free vitamin E. These findings demonstrate that surface amination enhanced the sustained-release behavior of the nanocellulose-based carrier. Both CNC-based formulations provided controlled release compared with free vitamin E, while Vit-E/CNC–NH_2 exhibited the most prolonged release profile, supporting the potential benefit of surface engineering for controlling vitamin E delivery.

3.6 | Release Kinetic Modeling

To further elucidate the mechanism governing vitamin E release from the developed nanocarriers, the experimental release data were fitted to zero-order, first-order, Higuchi, and Korsmeyer–Peppas kinetic models. The release profiles were further analyzed using zero-order, first-order, Higuchi, and Korsmeyer–Peppas kinetic models (*Fig. 3*). The corresponding kinetic parameters and coefficients of determination are summarized in *Table 4*.

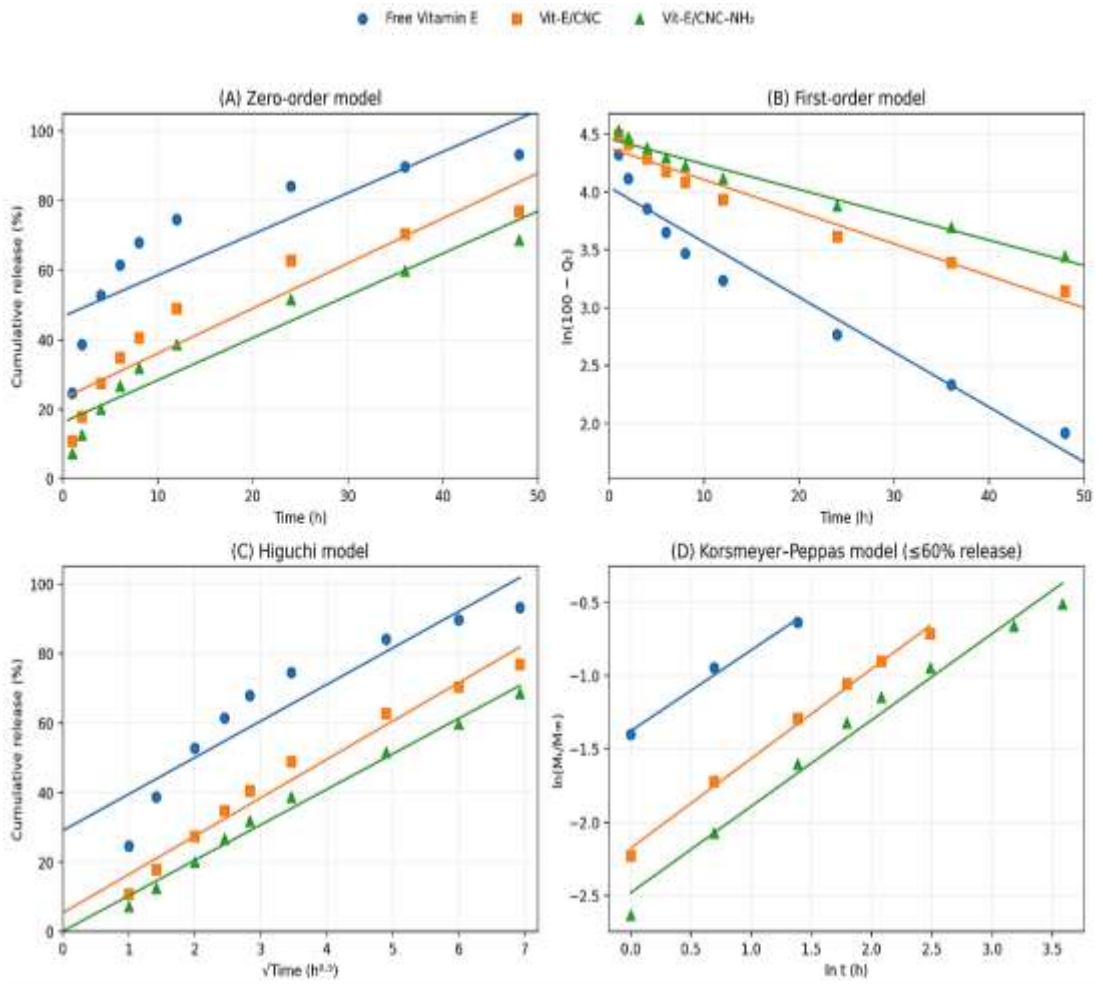

Fig. 3. Release kinetic modeling of free Vitamin E, Vit-E/CNC, and Vit-E/CNC–NH₂ using zero-order, first-order, Higuchi, and Korsmeyer–Peppas models.

Table 4. Release kinetic parameters for free Vitamin E, Vit-E/CNC, and Vit-E/CNC–NH₂.

Formulation	Zero-order R^2	First-order R^2	Higuchi R^2	Korsmeyer–Peppas R^2	n
Free Vitamin E	0.719	0.947	0.871	0.989	0.551
Vit-E/CNC	0.869	0.964	0.970	0.995	0.610
Vit-E/CNC–NH₂	0.911	0.975	0.988	0.979	0.588

The kinetic analysis revealed that the release behavior of the vitamin E formulations was better described by diffusion-related and anomalous release models than by a simple zero-order mechanism. As summarized in *Table 4*, free Vitamin E showed the highest coefficient of determination with the Korsmeyer–Peppas model (R^2=0.989), followed by the first-order model (R^2=0.947). For Vit-E/CNC, the Korsmeyer–Peppas model provided the highest fitting quality (R^2=0.995), while the Higuchi model also showed a strong correlation (R^2=0.970). Similarly, Vit-E/CNC–NH₂ exhibited the highest fitting quality with the Higuchi model (R^2=0.988), followed closely by the first-order (R^2=0.975) and Korsmeyer–Peppas (R^2=0.979) models.

The relatively high R^2 values obtained with the Higuchi model for both nanocellulose-based formulations indicate that diffusion through the nanocellulose matrix contributed substantially to the release of vitamin E. The particularly high Higuchi correlation observed for Vit-E/CNC–NH₂ (R^2=0.988) suggests that diffusion remained an important mechanism following surface amination. At the same time, the strong Korsmeyer–Peppas correlations observed for Vit-E/CNC (R^2=0.995) and Vit-E/CNC–NH₂ (R^2=0.979) indicate that the release process was not governed exclusively by a single mechanism and that matrix-related effects may also have contributed to vitamin E transport.

The Korsmeyer–Peppas exponent (n) provided additional information regarding the release mechanism. The calculated n values were 0.551 for free Vitamin E, 0.610 for Vit-E/CNC, and 0.588 for Vit-E/CNC–NH_2. The n values obtained for the two nanocellulose-based formulations fall within the range generally associated with anomalous or non-Fickian release under the commonly applied interpretation of the Korsmeyer–Peppas model. This behavior suggests that vitamin E release was influenced by a combination of diffusion and matrix-related processes rather than by simple Fickian diffusion alone.

Interestingly, the n value of Vit-E/CNC–NH_2 (0.588) was slightly lower than that of Vit-E/CNC (0.610), indicating that surface amination did not increase the contribution of matrix relaxation to the release process. Instead, the modified surface appears to have altered the balance between diffusion, hydration, and vitamin E–carrier interactions. The stronger retention of vitamin E within the aminated nanocellulose matrix, together with its lower cumulative release over 48 h, may reflect enhanced interactions between the loaded compound and the functionalized carrier surface.

The kinetic analysis indicates that vitamin E release from the nanocellulose-based systems involved substantial diffusion through the carrier matrix together with additional matrix-related effects. The high fitting coefficients obtained for the Higuchi and Korsmeyer–Peppas models, particularly for Vit-E/CNC–NH_2, support the ability of surface amination to modify the release behavior of nanocellulose and contribute to a more sustained delivery of vitamin E.

3.7 | Antioxidant Activity of Vitamin E-Loaded Nanocarriers

The antioxidant activity of free vitamin E and vitamin E-loaded nanocarriers was evaluated using the DPPH radical-scavenging assay. The percentage of DPPH radical inhibition was determined at different concentrations of vitamin E equivalents. The results are summarized in *Fig. 4*.

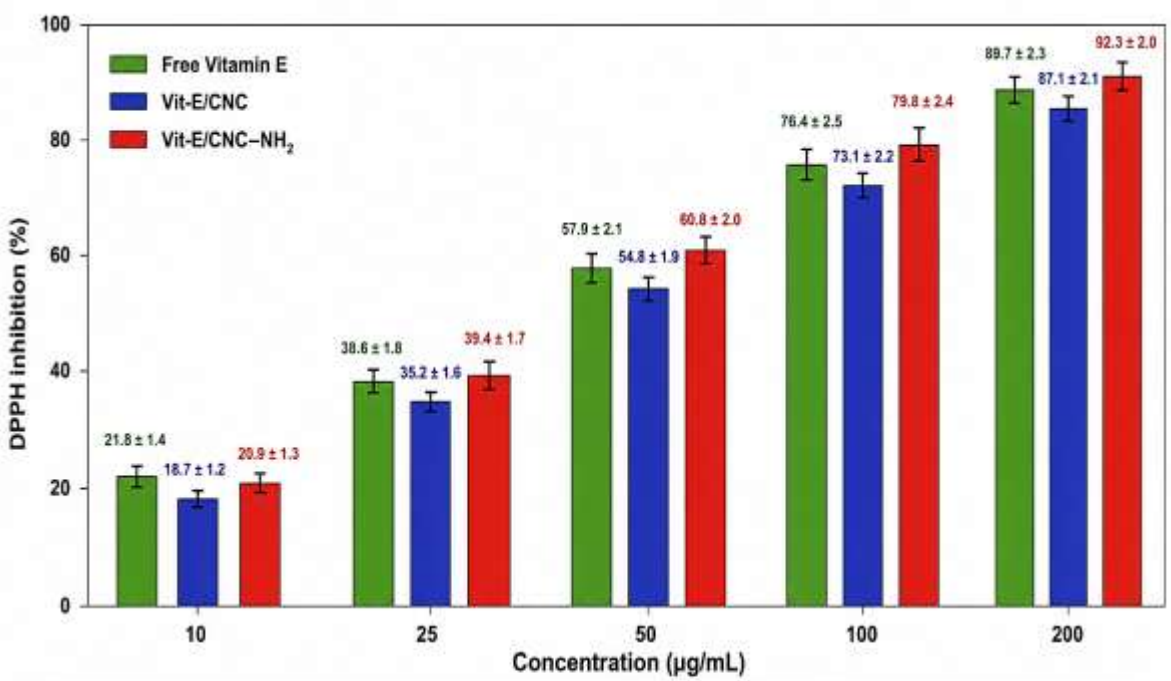

Sample	Concentration (µg/mL)				DPPH inhibition (%)	
	10	25	50	200		
Free Vitamin E	21.8 ± 1.4	38.6 ± 1.8	57.9 ± 2.1	76.4 ± 2.5	36.4 ± 2.5	89.7 ± 2.3
Vit-E/CNC	18.7 ± 1.2	35.2 ± 1.6	54.8 ± 1.9	73.1 ± 2.2	73.1 ± 2.2	87.1 ± 2.1
Vit-E/CNC–NH_2	20.9 ± 1.3	39.4 ± 1.7	60.8 ± 2.0	60.8 ± 2.0	79.8 ± 2.4	92.3 ± 2.0

Fig. 4. DPPH radical-scavenging activity of free vitamin E and vitamin E-loaded nanocarriers.

The antioxidant activity of free vitamin E, Vit-E/CNC, and Vit-E/CNC–NH_2 was evaluated using the DPPH radical-scavenging assay. As shown in *Fig. 4*, all vitamin E-containing formulations exhibited concentration-dependent antioxidant activity, with increasing DPPH radical inhibition observed as the vitamin E concentration increased. Free vitamin E exhibited DPPH inhibition values ranging from 21.8±1.4% to 89.7±2.3% over the concentration range of 10–200 μg/mL. Incorporation of vitamin E into CNC resulted in a slight reduction in the measured antioxidant activity, particularly at the lower concentrations. Nevertheless, Vit-E/CNC maintained substantial radical-scavenging activity, reaching 87.1±2.1% inhibition at 200 μg/mL. Interestingly, the aminated nanocarrier exhibited antioxidant activity comparable to or slightly higher than that of free vitamin E at higher concentrations. Vit-E/CNC–NH_2 demonstrated 60.8±2.0%, 79.8±2.4%, and 92.3±2.0% DPPH inhibition at 50, 100, and 200 μg/mL, respectively. The higher apparent activity of Vit-E/CNC–NH_2 compared with Vit-E/CNC may be associated with improved dispersion of vitamin E within the aqueous assay medium and more effective exposure of the active compound to the radical species. The relatively small difference between free vitamin E and Vit-E/CNC–NH_2 suggests that the loading process did not substantially impair the antioxidant functionality of vitamin E. This finding is particularly relevant because excessive interaction between an active compound and a carrier can sometimes reduce the accessibility of the active groups responsible for biological activity. The preservation of antioxidant activity, combined with the improved EE and sustained release profile observed for Vit-E/CNC–NH_2, indicates that surface-functionalized nanocellulose can serve as a promising carrier for vitamin E delivery. The ability of the system to maintain antioxidant activity while simultaneously providing controlled release represents an important advantage over the administration of free vitamin E. The results demonstrate that CNC–NH_2 successfully preserved the antioxidant activity of vitamin E while providing improved loading performance and sustained release, supporting its potential application as a nanocellulose-based delivery platform for vitamin E.

3.8 | Comparative Performance of Cellulose Nanocrystals and CNC–NH_2 as Vitamin E Nanocarriers

To provide an overall comparison of the developed nanocarriers, the main physicochemical and functional characteristics of CNC and CNC–NH_2 before and after vitamin E loading were compared. The summarized results are presented in *Table 5*.

Table 5. Comparative performance of unmodified and aminated nanocellulose as Vitamin E nanocarriers.

Parameter	CNC	CNC–NH_2	Relative Performance
Particle size (nm)	148.6±4.8	161.3±5.6	Comparable
PDI	0.218±0.019	0.231±0.021	Comparable
Zeta potential (mV)	−28.7±1.6	+21.6±1.8	Surface charge modified
Nitrogen content (%)	0.14±0.03	2.84±0.17	↑ Amination
EE (%)	76.8±1.7	87.9±1.5	+14.5%
LC (%)	5.1±0.1	5.9±0.1	+15.7%
48-h release (%)	76.9±2.9	68.7±2.8	More sustained
DPPH inhibition at 200 μg/mL (%)	87.1±2.1	92.3±2.0	Higher activity

The comparative analysis demonstrated that surface amination substantially improved the functional performance of nanocellulose as a vitamin E delivery system. Although CNC–NH_2 exhibited only a modest increase in particle size compared with unmodified CNC, its surface characteristics were markedly altered, as demonstrated by the increase in nitrogen content and reversal of zeta potential from negative to positive values. Most importantly, CNC–NH_2 exhibited a higher vitamin E EE (87.9±1.5%) compared with unmodified CNC (76.8±1.7%). The LC was also increased from 5.1±0.1% to 5.9±0.1% following amination. These findings suggest that surface functionalization improved the interaction and association of vitamin E with the nanocellulose carrier. The enhanced loading performance was accompanied by a more sustained release profile. After 48 h, Vit-E/CNC–NH_2 released 68.7±2.8% of the incorporated vitamin E, compared

with 76.9±2.9% for Vit-E/CNC. Thus, surface amination resulted in approximately 8.2 percentage points lower cumulative release over the experimental period. Importantly, the improved carrier performance did not compromise the antioxidant activity of vitamin E. At 200 μg/mL, Vit-E/CNC–NH_2 exhibited 92.3±2.0% DPPH inhibition, compared with 87.1±2.1% for Vit-E/CNC. This finding indicates that the modified carrier was capable of maintaining the functional activity of the loaded vitamin E while providing improved retention and controlled release. Taken together, these results demonstrate that surface engineering of nanocellulose with amine functionalities provided a clear functional advantage over unmodified CNC for vitamin E delivery. The CNC–NH_2 system combined high EE, improved LC, sustained release, and preserved antioxidant activity without substantially increasing particle-size heterogeneity.

4 | Conclusion

In the present study, aminated (CNC–NH_2) was developed and comparatively evaluated with unmodified CNC as nanocarriers for vitamin E delivery. Surface amination resulted in a substantial increase in nitrogen content and a pronounced change in surface charge, while maintaining the characteristic nanoscale morphology and crystalline structure of the nanocellulose. These findings confirmed that surface engineering successfully modified the interfacial properties of CNC without causing major structural disruption. The comparative formulation study demonstrated that CNC–NH_2 provided superior vitamin E loading performance compared with unmodified CNC, with higher EE and LC. Moreover, vitamin E-loaded CNC–NH_2 exhibited a more sustained release profile over 48 h, and kinetic analysis indicated an anomalous/non-Fickian release mechanism with a substantial diffusion contribution. Importantly, the antioxidant activity of vitamin E was effectively preserved following incorporation into the aminated nanocarrier. The findings suggest that amine functionalization represents an effective strategy for improving the performance of nanocellulose-based carriers for vitamin E delivery. Compared with native CNC, CNC–NH_2 provided a favorable combination of enhanced loading, controlled release, and preservation of antioxidant functionality [34–38]. Therefore, surface-engineered nanocellulose may represent a promising platform for the delivery of vitamin E and potentially other poorly water-dispersible bioactive compounds. Further studies involving long-term stability, cellular uptake, bioavailability, and in vivo evaluation are warranted to validate the practical potential of the developed system.

Authors' Contributions

The author was responsible for all stages of the research and manuscript preparation and approved the final version.

Funding

This research was not supported by any specific grant from funding bodies in the public, commercial, or not-for-profit sectors.

Data Availability

All data are included in the text.

Conflict of Interest

There are no competing interests to declare.

Consent for Publication

The author confirms consent for the publication of this work.

Ethics Approval and Consent to Participate

This article does not contain any studies with human participants performed by the author.

References

[1] Fatima, G., Dzupina, A., Mahdi, A. A., Fedacko, J., Magomedova, A., & Yousif, N. G. (2026). Role of vitamin-E as a vital nutrient in health and diseases. *Indian journal of clinical biochemistry*, *41*(3), 310–323. https://doi.org/10.1007/s12291-025-01309-0

[2] Kaye, A. D., Thomassen, A. S., Mashaw, S. A., MacDonald, E. M., Waguespack, A., Hickey, L., ... & Hickey, L. C. (2025). Vitamin E (α-tocopherol): Emerging clinical role and adverse risks of supplementation in adults. *Cureus*, *17*(2), e78679. https://doi.org/10.7759/cureus.78679

[3] Song, Y., Ni, W., Zheng, M., Sheng, H., Wang, J., Xie, S., ... & Shi, J. (2025). Vitamin E (300 mg) in the treatment of MASH: A multi-center, randomized, double-blind, placebo-controlled study. *Cell reports medicine*, *6*(2),101939. https://www.cell.com/cell-reports-medicine/fulltext/S2666-3791(25)00012-6

[4] Traber, M. G., & Sies, H. (1996). Vitamin E in humans: Demand and delivery. *Annual review of nutrition*, *16*(1), 321–347. https://doi.org/10.1146/annurev.nu.16.070196.001541

[5] Eggersdorfer, M., Schmidt, K., Péter, S., Richards, J., Winklhofer-Roob, B., Hahn, A., & Obermüller-Jevic, U. (2024). Vitamin E: Not only a single stereoisomer. *Free radical biology and medicine*, *215*, 106–111. https://doi.org/10.1016/j.freeradbiomed.2024.02.013

[6] Li, Y., Yang, D., Ren, Y., Luo, Y., Zheng, H., Liu, Y., ... & Zhang, L. (2025). Vitamin E in plants: Biosynthesis pathways, biofortification strategies, and regulatory dynamics. *International journal of molecular sciences*, *26*(7), 3380. https://doi.org/10.3390/ijms26073380

[7] Brown, B. G., & Crowley, J. (2005). Is there any hope for vitamin E? *JAMA*, *293*(11), 1387–1390. https://doi.org/10.1001/jama.293.11.1387

[8] Traber, M. G. (2007). Vitamin E regulatory mechanisms. *Annual review of nutrition*, *27*, 347–362. https://doi.org/10.1146/annurev.nutr.27.061406.093819

[9] Barani, D., Bouafia, A., Laouini, S. E., Tedjani, M. L., Alharthi, F., Sonia, M. T., & Trzepieciński, T. (2025). Enhanced antioxidant, anti-inflammatory, and photocatalytic properties of $α$-tocopherol-coated copper oxide nanoparticles: Synthesis, characterisation, and multifunctional applications. *International journal of food science and technology*, *60*(1), vvaf051. https://doi.org/10.1093/ijfood/vvaf051

[10] Kukri, A., Rossi, M., Freschi, L., Czékus, Z., & Poór, P. (2025). Phytohormonal regulation of $α$-tocopherol in plants. *Plant stress*, *18*, 101032. https://doi.org/10.1016/j.stress.2025.101032

[11] Goswami, R. K., & Verma, P. (2025). Production of α-tocopherol biomolecules using various cultivation strategies of diverse microalgal species: Purification, characterization and assessment of antioxidant properties. *Biocatalysis and agricultural biotechnology*, *67*, 103635. https://doi.org/10.1016/j.bcab.2025.103635

[12] Dudek, A., Spiegel, M., Benkowska-Biernacka, D., Domańska, M., & Pruchnik, H. (2025). Impact of $α$-tocopherol derivatives on the structural and functional properties of model lipid nanocarriers: A biophysical modeling study. *Chemistry and physics of lipids*, *272*, 105539. https://doi.org/10.1016/j.chemphyslip.2025.105539

[13] Santonastaso, M., Mottola, F., Iovine, C., Genualdo, V., Montano, L., Piscopo, M., ... & Rocco, L. (2025). Protective effects of anthocyanin and α-tocopherol against titanium dioxide nanoparticle-induced DNA damage in human sperm cells. *Exposure and health*, *17*(2), 523-535. https://doi.org/10.1007/s12403-024-00675-z

[14] Ijaz, M., Madni, A., Khan, H. M. S., Arshad, T., Meer, S., Ijaz, F., ... & Batiha, G. E. S. (2025). Nanostructured lipid carrier based gel containing α-tocopherol and α-tocopheryl acetate for synergistic cutaneous antiaging efficacy. *Scientific reports*, *15*(1), 42360. https://doi.org/10.1038/s41598-025-26277-6

[15] Amić, A., Milanović, Ž., & Cagardová, D. M. (2025). Protective roles of $α$-tocopherol, $α$-CEHC, and gallic acid against $CO_3^{\bullet-}$-induced DNA damage and their effect on OGG1 and pro-oxidant enzymes. *Journal of molecular liquids*, *438*, 128847. https://doi.org/10.1016/j.molliq.2025.128847

[16] López-Puebla, S., Arias-Santé, M. F., Romero, J., de Camargo, A., & Rincón-Cervera, M. Á. (2025). Analysis of fatty acid profile, $α$-tocopherol, squalene and cholesterol content in edible parts and by-products of south pacific wild fishes. *Marine drugs*, *23*(3), 104. https://doi.org/10.3390/md23030104

[17] Müller-Carneiro, J., de Freitas Rosa, M., Rodrigues, C., Freire, F., Steubing, B., & de Figueirêdo, M. C. B. (2025). Scenario-based life cycle assessment of cellulose nanocrystals production from agro-industrial by-products in 2040. *Journal of cleaner production*, *522*, 146238. https://doi.org/10.1016/j.jclepro.2025.146238

[18] Santos Samaritano Pereira, M. (2025). 945 efficacy evaluation of cellulose nanocrystals in sustainable surgical materials: A systematic review and meta-analysis. *British journal of surgery*, *112*(Supplement_10), znaf128-120. https://doi.org/10.1093/bjs/znaf128.120

[19] Forssell, S., Pääkkönen, T., Tirronen, E., Kontturi, E., & Oinas, P. (2026). Techno-economic and life cycle assessment of carboxylated cellulose nanocrystals production on industrial scale. *ACS sustainable chemistry & engineering*, *14*(1), 47–56. https://doi.org/10.1021/acssuschemeng.5c02062

[20] Arockiasamy, F. S., Manoharan, B., Santhi, V. M., Prakalathan, K., Periasamy, D., Dhandapani, A., ... & Ilyas, R. A. (2025). Navigating the nano-world future: Harnessing cellulose nanocrystals from green sources for sustainable innovation. *Heliyon*, *11*(1). https://www.cell.com/heliyon/fulltext/S2405-8440(24)17219-2

[21] Sonowal, D., & Wani, K. M. (2025). Comprehensive review of cellulose nanocrystals: Preparation, properties, modifications and applications. *Bulletin of the national research centre*, *49*(1), 55. https://doi.org/10.1186/s42269-025-01349-9

[22] Dagnino, E. P., Ehman, N., & Area, M. C. (2025). Recent advances in cellulose nanocrystal production from green methods. *Processes*, *13*(3), 790. https://doi.org/10.3390/pr13030790

[23] Rajendran, N., Runge, T., Bergman, R., Nepal, P., Ali, S. D., Al Fahim, A., & Moradllo, M. K. (2025). Economic and environmental impact analysis of cellulose nanocrystal-reinforced cementitious mixture in 3D printing. *Resources, conservation and recycling*, *218*, 108252. https://doi.org/10.1016/j.resconrec.2025.108252

[24] Layek, S., & Sarkar, N. (2025). Emerging trends and future perspectives in luminescent cellulose nanocrystals. *Langmuir*, *41*(45), 30043–30050. https://doi.org/10.1021/acs.langmuir.5c02840

[25] Baniasad, A., Baei, M. S., & Tala-Tapeh, S. M. (2025). Chitosan-PEGylated niosomes and liposomes as biomacromolecule carriers for Alzheimer's disease treatment: Galantamine drug delivery carrier. *Materials chemistry and physics*, *352*, 132003. https://doi.org/10.1016/j.matchemphys.2025.132003

[26] Abdelkader, R. S., Helal, G. A., Galal, Y. G. M., Soliman, S. M., Khalil, R. R., & Elsayed, N. (2025). New trends in mycosynthesis of cellulose nanocrystals promoted by gamma irradiation of sugarcane bagasse. *International journal of environmental science and technology*, *22*(9), 7867–7884. https://doi.org/10.1007/s13762-024-06144-z

[27] Sharma, V. S., Mishra, S., Sharma, A. S., Sharma, N., Varma, R. S., Shrivastav, P. S., & Ammathnadu Sudhakar, A. (2025). Microcrystalline cellulose and cellulose nanocrystals: Ecofriendly and sustainable support materials in heterogeneous nanocatalysis for green organic transformations. *Asian journal of organic chemistry*, *14*(2), e202400586. https://doi.org/10.1002/ajoc.202400586

[28] Niknejad, K., Sharifzadeh, B. M., & Motallebi, T. T. S. (2018). Synthesis of Metformin Hydrochloride nanoliposomes: Evaluation of physicochemical characteristics and release kinetics. *International journal of nano dimension, 9*(3), 298-313. (**In Persian**). https://www.sid.ir/paper/322408/en

[29] Kaur, N., Hamid, Dash, K. K., Choudhary, P., & Shams, R. (2025). Sustainable and versatile applications of cellulose nanocrystals in food processing: A comprehensive review. *Polymer bulletin*, *82*(14), 8763–8789. https://doi.org/10.1007/s00289-025-05894-1

[30] Wang, S., Du, W., Liu, W., Li, J., Yi, Z., Chen, Z., ... & Li, M. (2025). Machine learning-driven prediction and optimization of microcrystalline cellulose and cellulose nanocrystal production from Miscanthus biomass. *Industrial crops and products*, *237*, 122180. https://doi.org/10.1016/j.indcrop.2025.122180

[31] Raghuwanshi, V. S., & Garnier, G. (2025). Nanoparticle decorated cellulose nanocrystals (CNC) composites for energy, catalysis, and biomedical applications. *Advanced functional materials*, *35*(2), 2412869. https://doi.org/10.1002/adfm.202412869

[32] Nicastro, G., Fahimi, A., Dufresne, A., Vahidi, E., Punta, C., & Bontempi, E. (2025). Eco-design of cellulose nanocrystals through ESCAPE method at lab-scale. *Carbohydrate polymers*, *369*, 124310. https://doi.org/10.1016/j.carbpol.2025.124310

[33] Putra, N. R. (2025). Advances in cellulose composite films for sustainable food packaging: A review. *Nordic pulp & paper research journal*, *41*(1). https://doi.org/10.1515/npprj-2025-0038

[34] Wang, S., Yu, Z., Sun, X., Panahi-Sarmad, M., Yang, P., Zhu, P., ... & Jiang, F. (2025). A universal strategy to mitigate microphase separation via cellulose nanocrystal hydration in fabricating strong, tough, and fatigue-resistant hydrogels. *Advanced materials*, *37*(7), 2416916. https://doi.org/10.1002/adma.202416916

[35] Xu, J., Dong, Q., Liu, P., Cai, Z., & Liu, D. (2025). Rheology of cellulose nanocrystals dispersed in dimethyl sulfoxide. *Carbohydrate polymers*, *369*, 124300. https://doi.org/10.1016/j.carbpol.2025.124300

[36] Nozick, V. (2026). Engineering and characterization of acyclovir-loaded nano-niosomes for enhanced antiviral drug delivery. *Nano nexus & applications*, *1*(2), 95–105. https://doi.org/10.48314/nna.vi.66

[37] Baniasad, A. (2026). Role of silk fibroin in modulating thermo-responsive behavior of PNIPAM hydrogels. *Biocompounds*, *3*(1), 54–62. https://doi.org/10.48313/bic.vi.62

[38] Javad, M. P. M., Reza, M. S. H., Simin, D., Ahmed, E. S., Bahram, B., & Azadeh, H. (2014). Preparation and evaluation of the antiviral activity of acyclovir loaded nano-niosomes against herpes simplex virus type 1. *Pharmacophore*, *5*(4–2014), 483–493. https://pharmacophorejournal.com/cI958b4?